Accelerator Department

BROOKHAVEN NATIONAL LABORATORY
Associated Universities, Inc.

EP&S DIVISION TECHNICAL NOTE

NO. 90

H. Brown

June 2, 1980

A TIME SEPARATED $\bar{p}$ BEAM

A Time Separated $\bar{p}$ Beam

I. Introduction

In 1974, Fainberg and Kalogeropoulos[1] measured the time structure of a resonant extracted beam from the AGS with the RF kept on to maintain tight bunching. The external pulses were found to be unexpectedly narrow (FWHM = 2.4 nsec after correction for counter resolution). An explanation for this and some pertinent comments were put forth by Barton[2] in a subsequent report.

The original motivation for the study was to examine the extent to which single counter time of flight (TOF) measurements would be feasible, making it possible to measure velocities of neutral secondary particles from a target.[3] The encouraging result led later to a proposal by Kalogeropoulos[4] to use the tightly bunched protons to produce a secondary time separated beam (TSB) of anti-protons, i.e., a beam with a long flight path over which the lower velocity particles ($\bar{p}$'s) separate longitudinally from the more numberous fast particles (π's) so that the $\bar{p}$ interactions can be studied independently by suitably gated detectors.

II. TOF Characteristics

For a given beam length L, there are various momenta p at which the $\bar{p}$ TOF is equal to the π^- TOF plus an integral number of AGS bunch periods:

$$t_{\bar{p}} = t_{\pi} + n\,T$$

i.e., $\bar{p}$'s of these flight times are overlapped by the intense π^- bursts from later bunches striking the target. If the effective π^- pulse width is $\pm\,\delta$, then there are overlap bands given by

$$\Delta(p,L) \equiv (t_{\bar{p}} - t_{\pi}) = n\,T \pm \delta \qquad (1)$$

within which beam particles are unusable and the experimental detectors are to be vetoed. For n = 0, only $\Delta = +\delta$ has significance. The function Δ is:

$$\Delta(p,L) = \frac{L}{c}\left(\frac{1}{\beta_{\bar{p}}} - \frac{1}{\beta_{\pi}}\right) = \frac{L}{c}\left(\frac{E_{\bar{p}} - E_{\pi}}{pc}\right) \tag{2}$$

$$= \tau\left[\sqrt{1+\left(\frac{m_{\bar{p}}c}{p}\right)^2} - \sqrt{1+\left(\frac{m_{\pi}c}{p}\right)^2}\right]\left\{\tau = \frac{L}{c}\right\}$$

and the inverse of this is

$$\frac{a^2c^2}{p^2} = \frac{\Delta}{\tau}\left[\frac{\Delta}{\tau}\,\frac{b^2}{a^2} + 2\sqrt{1+\left(\frac{\Delta}{\tau}\right)^2\left(\frac{m_{\bar{p}}m_{\pi}}{a^2}\right)^2}\right] \tag{3}$$

$$\left\{a^2 = \left(m_{\bar{p}}^2 - m_{\pi}^2\right) > 0,\ b^2 = \left(m_{\bar{p}}^2 + m_{\pi}^2\right),\ \tau = \frac{L}{c}\right\}$$

Fainberg and Kalogeropoulos[1] show that the AGS bunch may be adjusted so that, including the resolving time of their detecting circuit, the proton density falls off as $e^{\frac{-t}{\tau_B}}$, where $\tau_B = 3.7$ nsec, on either side of bunch center. Using their detector as a practical example, and taking the position that we want the overlapping π^- intensity to be down by a factor of $r = 10^3$, we would set

$$\delta = \tau_B\,(\ln r) = 25.6 \text{ n sec.} \tag{4}$$

in Equation (1).

To the extent that the pion decay helps to purify the beam, the overlap bands would tend to become narrower with increasing decay length L. If one could effectively remove the resultant muons at the end of the beam, then in such an ideal case the overlap band widths would taper to zero, and remain so, where

$$e^{-\frac{L}{c\tau_{\pi}}\,\frac{m_{\pi}c}{p}} \leq \frac{1}{r}\left\{\tau_{\pi} = \text{pion lifetime}\right\}$$

Equation (4) would be replaced by

$$\delta = \tau_B \left[\ln r - \frac{L}{c\tau_\pi} \quad \frac{m_\pi c}{p} \right] \gtrless 0 \qquad (5)$$

Substituting this in Equation (1), the overlap bands may be calculated from (2) or (3). They are shown in Fig. 1. Without the pion decay, each overlap band would have an approximately uniform width on the log-log plot.

III. The Long Transport Section

Since Fig. 1 indicates that a TSB will be hundreds of meters in length, an economical optical system must be designed to transport a large phase space over a long distance. Given the 28 eight inch aperture quadrupoles that we will obtain from SREL, this is not a difficult problem, in principal, since a simple alternating gradient channel (AGC) can accept a relatively large transverse phase space over a substantial momentum band, say $\pm$ 10% or more. A plot of the betatron oscillation function β_{max} (at the center of a focussing quad) versus quadrupole focal strength exhibits a very broad minimum; i.e., the acceptance $E = \pi \frac{a^2}{\beta_{max}}$ varies slowly over a wide range of momenta. This behaviour is illustrated in Fig. 2, which is drawn for the case of thin lenses (a good approximation for the channels of interest here). We see that if the quads are spaced by a distance ℓ on centers, $\beta_{max}/\ell \doteq 3.35$. Hence, the acceptance in the initially focussing plane is

$$E_f = \pi \frac{a^2}{3.35\ell}$$

where a = quad aperture radius.

In the other plane, there is more variation in the aspect ratios of the (upright) admittance ellipses, but nevertheless, over $\pm$ 10% in momentum, the common area accepted is still about 90% of E_f.

The total transverse acceptance of the AGC is then

$$E_f E_d \doteq (.9) \left(\frac{\pi}{3.35}\right)^2 \frac{a^4}{\ell^2}$$

If the source has semi-widths of w_x and w_y and emits into semi-angles $\Delta x'$ and $\Delta x'$, then equating source emittance to channel admittance, we have

$$(\pi w_x \Delta x')(\pi w_y \Delta y') = E_f E_d \doteq (.9) \frac{\pi^2}{(3.35)^2} \left(\frac{a^2}{\ell}\right)^2$$

The accepted solid angle is therefore:

$$\Delta\Omega = \pi \Delta x' \Delta y' \doteq \frac{.9\pi}{(3.35)^2} \left(\frac{a^2}{w_x w_y}\right) \left(\frac{a}{\ell}\right)^2 \qquad (7)$$

As an example, suppose we distribute the 30 quads over 300 meters, then $\ell \doteq$ 400" while a = 3.75". A typical AGS target corresponds to $w_x\ w_y$ = 0.1" x 0.05". This leads to $\Delta\Omega$ = 62 mster which, multiplied by a momentum band of $\pm$ 10% or so, would mean a very substantial acceptance. The catch is encountered in trying to perform the emittance match implicit in Eq.(7) over a wide momentum range; the actual acceptance realized is much smaller. This problem will be discussed further in Section V.

As pointed out by Kalogeropoulos, the TSB momentum range need not be restricted to the range between the n = 0 and n = 1 boundaries of Fig. 1. The n = 1 and n = 2 overlap bands are separated by about $\Delta p/p = \pm$ 15%, while $\Delta p/p = \pm$ 9% is the n = 2 to n = 3 separation. Thus, if the transport system is arranged to select momentum bites less than these amounts, the beam may be used at momenta below the n = 1 overlap band.

IV. Momentum Selection

A unit cell with a phase shift of $\pi/2$ lies near the broad minimum in β_{max}. Selecting this phase shift for the AGC allows one to neatly embed two equal bend dipoles early in the lattice, separated by $\Delta\Psi = \pi$, with a Δp defining slit at $\Delta\Psi \doteq \pi/2$. The remainder of the channel is then approximately adispersive. The momentum recombination is not exact, of course, due to the chromatic aberration in the quads. The effect of the residual dispersion was observed in the particle loss pattern, downstream of the dipoles, in the Monte Carlo calculations of Section VII.

A bend in the beam line is also imperative to prevent an intense proton beam from entering the AGC. The proton separation can also be aided by employing a non-zero (0.5°-1.0°) $\bar{p}$ production angle. After the proton beam separates from the negative TSB, it can be dumped in a beam stop or, at some expense, deflected out to another target location.

In section II, it was remarked that pion decay could help to purify the beam if the resulting muons could be removed. This could be largely accomplished by means of another momentum defining section, at the end of the AGC, similar to the one just described. Such a section has not been included in the examples below because it is quite likely that some users will wish to have an even higher resolution arrangement for the purpose of measuring individual incoming particle momenta. The details of such a beam spectrometer will be experiment dependent and have not been studied carefully as yet.

V. The Entrance Doublet

In Section III, it was mentioned that it is difficult to effect an exact match over a wide momentum band from a small, large solid angle source into an AGC with large aperture and small angular spread. Monte Carlo beam traces were performed to determine how many $\bar{p}$'s could be captured in the channel's acceptance. An exact matching (at $p = p_o$) arrangement of three or four suitably placed quads (with apertures arbitrarily large) was found to exhibit very severe chromatic aberration. The overall emittance into the acceptance of the quad channel was less than that from a simple doublet focussed for a point to parallel condition in both planes. ($H_{22} = V_{22} = 0$). Consequently, such a doublet was chosen as the basic objective lens for the system.

An attempt was made to correct the chromatic aberration of the objective doublet by inserting sextupoles and additional dipoles in the first 4 cells ($\Delta\Psi = 2\pi$) of the transport channel. This approach was suggested by a method

devised by K. Brown[5] to eliminate the 2nd order chromatic (momentum-dependent) terms in a curved AG lattice. Using the program TRANSPORT,[6] it was possible to make various ($\delta p \delta \xi_T$) terms of the second order transformation matrix go to zero or, alternatively, to minimize the effects of these terms on an ellipsoid representing the $\bar{p}$ emittance. Although the method works very nicely for the chromatic aberration arising in the lattice itself, it did not seem to be effective in reducing the chromatic effect of the objective doublet, which is the dominant source in this case. In fact, all the "solutions" obtained for the sextupole scheme led to lower fluxes, eventually transported through the remainder of the channel, then were obtained with no sextupoles and only two bends for momentum selection-recombination. In addition, a "gentler" match, combining the quads in the first two cells of the AGC with the doublet, was also tried, again with inferior results.

For given maximum pole tip fields and apertures, the optimum doublet configuration depends on momentum, with longer quads required for higher momenta. In an attempt to approximate the optimum doublet over a range of momenta, the front ends of the example beams described here have four quadrupoles at the front end. The scheme then, is to use Q1 and Q2 as the collecting doublet at the lowest momenta, with Q3 and Q4 set to some "neutral" condition. ("Neutral" is hazily defined as some set of fields which tends to minimize spreading of the p beam before it enters the quad channel. This point hasn't been investigated yet, and so, in the example beams described, the fields were set to zero.) For intermediate momenta, the first element of the doublet would be (Q1,Q2) together, with Q3 being the second element and with Q4 off. The highest momenta would require the doublet to be (Q1,Q2,Q3), Q4. This works out fairly well since, for the point to parallel condition, the first element of this doublet must be donsiderably stronger than the second.

VI. Spot Focus at Experiment

The final beam spot is formed simply by adding another doublet at the end of the AGC. Since the beam emittance is largest in the vertical plane, the final doublet element was chosen to be vertically focussing for the example beams discussed in the next section. The same doublet was used for both examples for simplicity. It gives a convenient spot size in both cases. The final beam length and momentum range chosen, and experimental needs, would lead to a closer optimization of this doublet.

VII. Example Beams

In order to illustrate the range of possibilities, two AGC examples have been chosen, one with quads spaced 400" on centers and one with them 1200" on centers. Table I lists some pertinent data for the two examples. A conception of the layout of the shorter beam is shown in Fig. 3.

The fourth objective lens, Q4, is horizontally focussing and incorporates the function of the first half quad (½QH1) of the AGC. Similarly, the last AGC quad (½QH16) is included in the 8Q32 which also forms Q5 of the spot focussing doublet. The AGC quads QV1, QH2, and QV2 have 12" apertures to allow for the momentum dispersion in those two cells. Consequently, the 15 cells of the AGC utilize just 26 distinct quads of the 8Q16 or 8Q24 varieties and 3 of the 12Q30 or 12Q40 varieties.

The acceptances ($\Delta\Omega\Delta p/p$) for these two examples, derived from Monte Carlo ray tracing, are illustrated in Figures 4 and 5. In each figure, the continuous curve for the "Optimum Doublet" is derived using two quads operating at maximum pole tip field (assumed to be 3.6 kG/inch x 4.0 inch = 14.4 kG) whose lengths are set differently at each momentum to produce the point to parallel condition desired. The real, fixed length quads employed as described in Section V, produce the stepped acceptances shown. Naturally, on each step, the gradients increase proportionally with p until the maximum

(3.6 kG/inch) is reached, at which point one must step down and use the next longer quad combination. Corresponding $\bar{p}$ yields, calculated from the Sanford-Wang production formula,[7] are shown in Fig. 6. The formula is not reliable below $\sim$ 2.0 GeV/c.

VIII. Alignment and Other Constraints

One must be careful in positioning the quadrupoles in a long alternating gradient channel. For the limited number of cells chosen, 15, the tolerances are stringent but not overly severe. If all quads are randomly positioned with the same rms error, δ_{rms}, then the rms phase space (x,x' say) displacement of the beam axis at the end of the AGC (½QH16) is on a very nearly upright ellipse with amplitudes

$$\delta x_{rms} = 14.7\ \delta_{rms}$$

$$\delta x'_{rms} = 4.31\ \left(\delta_{rms}/\ell\right)$$

where ℓ is the center to center quad spacing.

If all quads are misaligned in the appropriate phase by an amount $\pm\ \delta$, then the maximum beam displacements at the end of the AGC are:

$$\begin{pmatrix} \delta x_{max} \\ \delta x' \end{pmatrix} = \begin{pmatrix} 59.8\ \delta \\ 11.7\ \delta/\ell \end{pmatrix} \quad \{\text{for max } \delta x\}$$

or

$$\begin{pmatrix} \delta x \\ \delta x'_{max} \end{pmatrix} = \begin{pmatrix} 40.0\ \delta \\ 17.5\ \delta/\ell \end{pmatrix} \quad \{\text{for max } \delta x'\}$$

The vertical effects at the center of the last vertically focussing quad would be slightly smaller.

Hence, if δ_{rms} = 0.02", the rms displacement near the end of the AGC would be about 0.3" or 8% of the aperture and we would begin to notice a loss of flux. An unfortunate in-phase error of $\pm$ 0.02" could lead to a 1.2" excursion.

Finally, one should note that, from the presently envisaged "D" target position, it is 490 meters to the ISABELLE ring. The long example beam, 924 m, would have to include a vertical rise of perhaps 2 meters in order to be able to pass the TSB beam pipe over the ISABELLE ring tunnel. The AGC quad spacing would have to be tailored to span the cross-over point. Beyond that, to the north, one would have to cope with the recharge basin. There would undoubtedly be a number of other problems. The longest TSB, allowing for an experimental area and muon stop, that could be installed without serious interaction with ISABELLE would be about 450 meters long. Any TSB over $\sim$ 200 m in length will have to make a cut up to $\sim$ 18 feet deep in the hill lying between 5th Avenue and the ISA. It may be preferable to translate the TSB elevation. For instance, two 2° pitching magnets could provide a 10 foot rise over 4 unit cells ($\Delta\psi = 2\pi$), leaving the beam dispersion-free thereafter. There would be some beam loss between the pitchers, but this could be minimized by placing them near horizontally focussing quads.

References

1. A. Fainberg and T. Kalogeropoulos, "The AGS Beam Structure", Accelerator Dept. Informal Report BNL-18938, May 6, 1974.

2. M.Q. Barton, "Some Comments on AGS Bunch Areas", Accelerator Dept. Informal Report, BNL-19076, July 17, 1974.

3. T. Brando, A. Fainberg, T. E. Kalogeropoulos, D. N. Michael, G. S. Tzanakos, "Observation of Low Energy Anti-neutrons in a Time Separated Neutral Beam at the AGS", Dept. of Physics, Syracuse University (to be published).

4. Private Communication and Letter of Intent.

5. Private Communication.

6. K.L. Brown, F. Rothacker, D.C. Carey, Ch. Iselin, "Transport - A Computer Program for Designing Charged Particle Beam Transport Systems", SLAC-91, Rev. 2, May 1977.

7. J. R. Sanford and C. L. Wang, "Empirical Formulas for Particle Production in P-Be Collisions Between 10 and 35 GeV/c", Accelerator Department AGS Internal Report JRS/CLW-2, May 1, 1967.

TABLE I: EXAMPLE BEAMS

Overall Length:	314 m	924 m
Objective Lenses:	3 ea-8Q24	3 ea-8Q32
	1 ea-8Q32	1 ea-8Q48
AGC Lattice:	15 cells	15 cells
	400" on Centers	1200" on Centers
AGC Quads:	26 ea-8Q26 (or 8Q24)	26 ea-8Q16(24)
	3 ea-12Q30 (or 12Q40)	3 ea-12Q30(40)
Dipole Bends:	2 ea-18D36, 2° each	2 ea-18D36, 2/3° each
Spot Focus:	1 ea-8Q32	1 ea-8Q32
	1 ea-8Q48	1 ea-8Q48
Spot: RMS Widths	.44"H x .17" V	.18"H x .08"V
Base Widths	2.4"H x 0.8"V	1.2"H x 0.7"V
Separable p	∿ 1.5 - 4.2 GeV/c	∿ 2.7 - 7.8 GeV/c
	∿ 1.0 - 1.1 GeV/c	∿ 1.8 - 2.15 GeV/c
	∿ 0.8 GeV/c	∿ 1.47 GeV/c
Acceptances: $\Delta\Omega\Delta p/p$	1.47 msr	0.35 msr
	0.72 msr	0.26 msr
	0.42 msr	0.16 msr

GRAPH PAPER GRAPHIC CONTROLS CORPORATION Buffalo, New York
Printed in U.S.A.
LOGARITHMIC 2 X 3 CYCLES AL-2451-BF

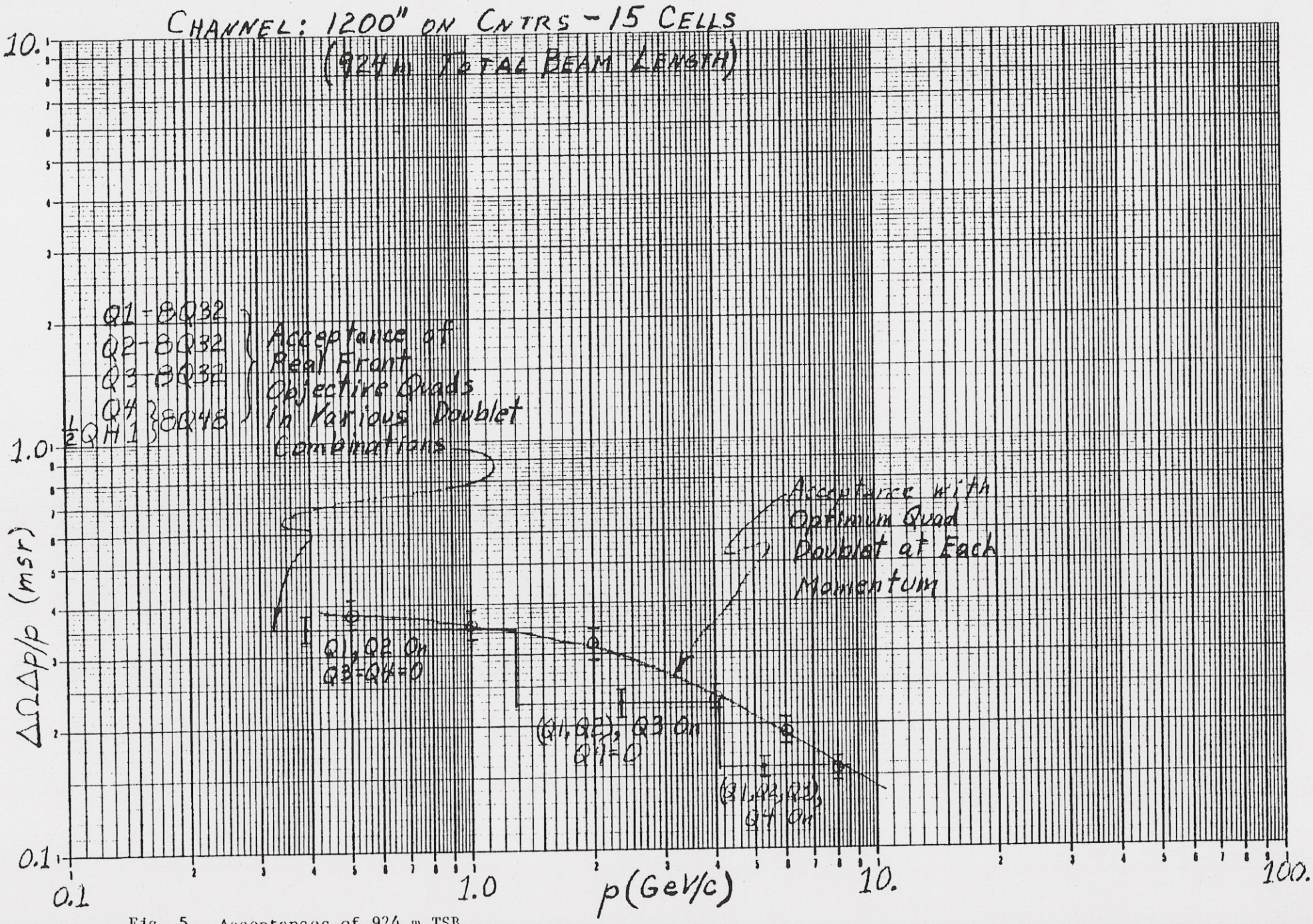

Fig. 5. Acceptances of 924 m TSB

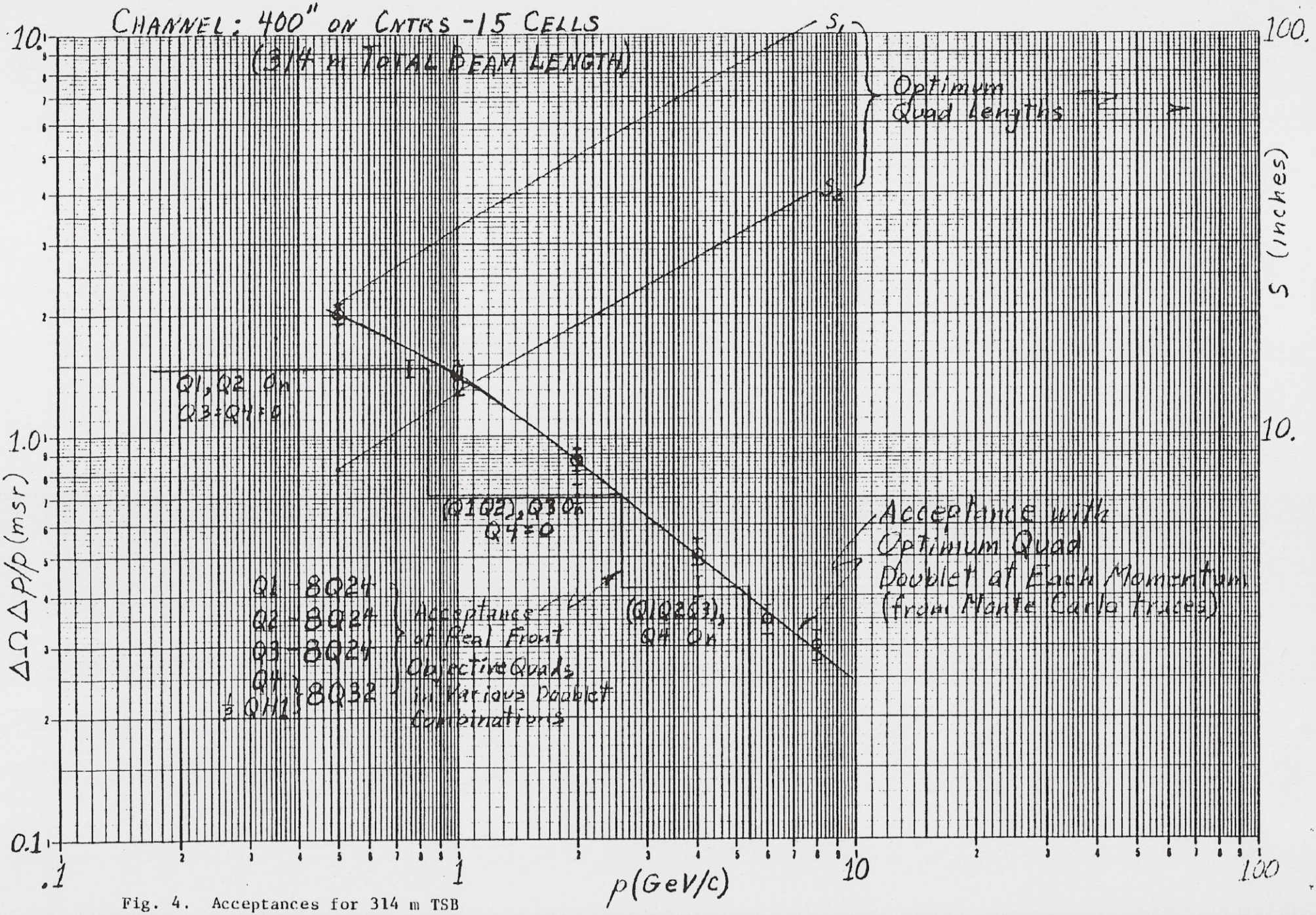

Fig. 4. Acceptances for 314 m TSB

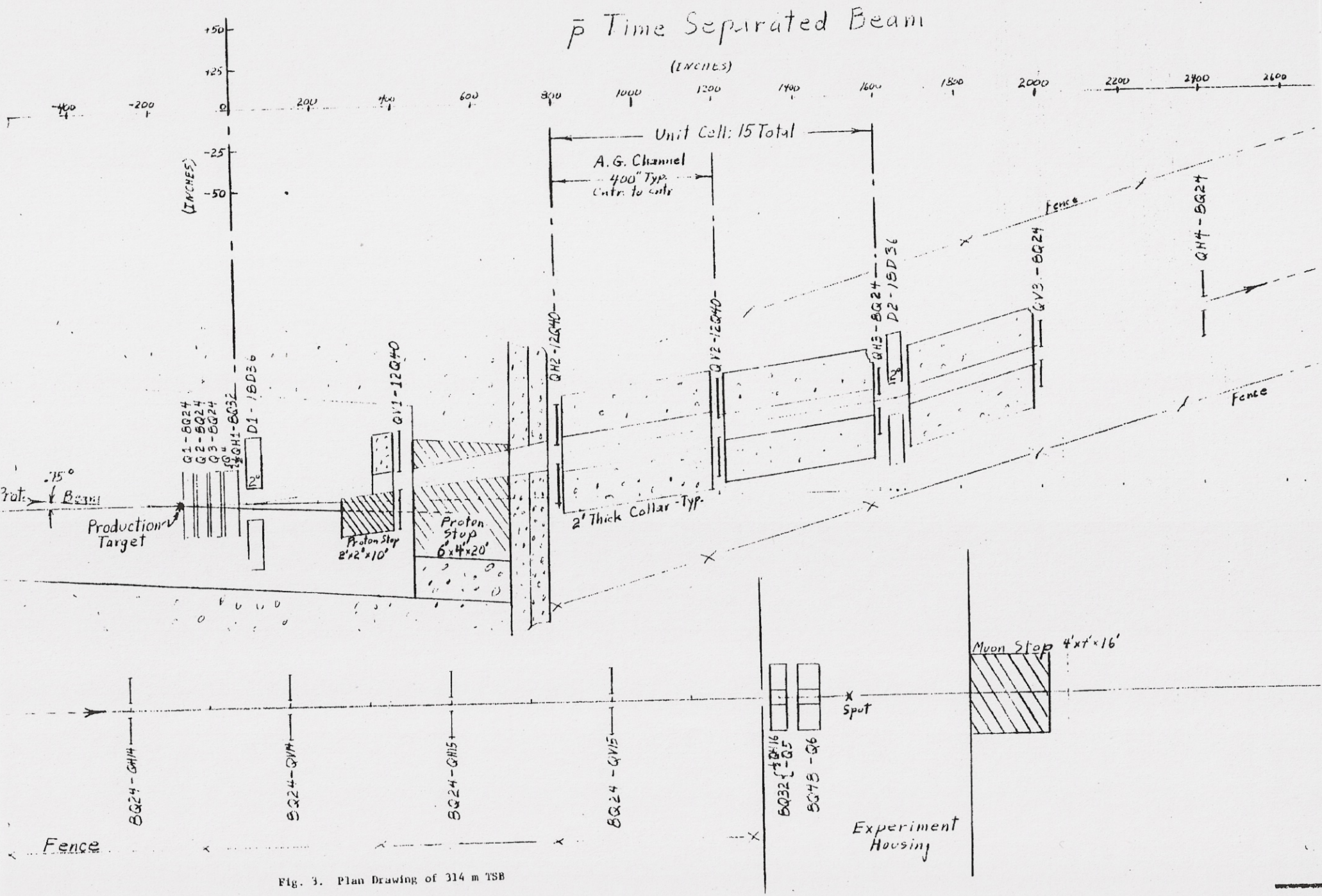

Fig. 3. Plan Drawing of 314 m TSB

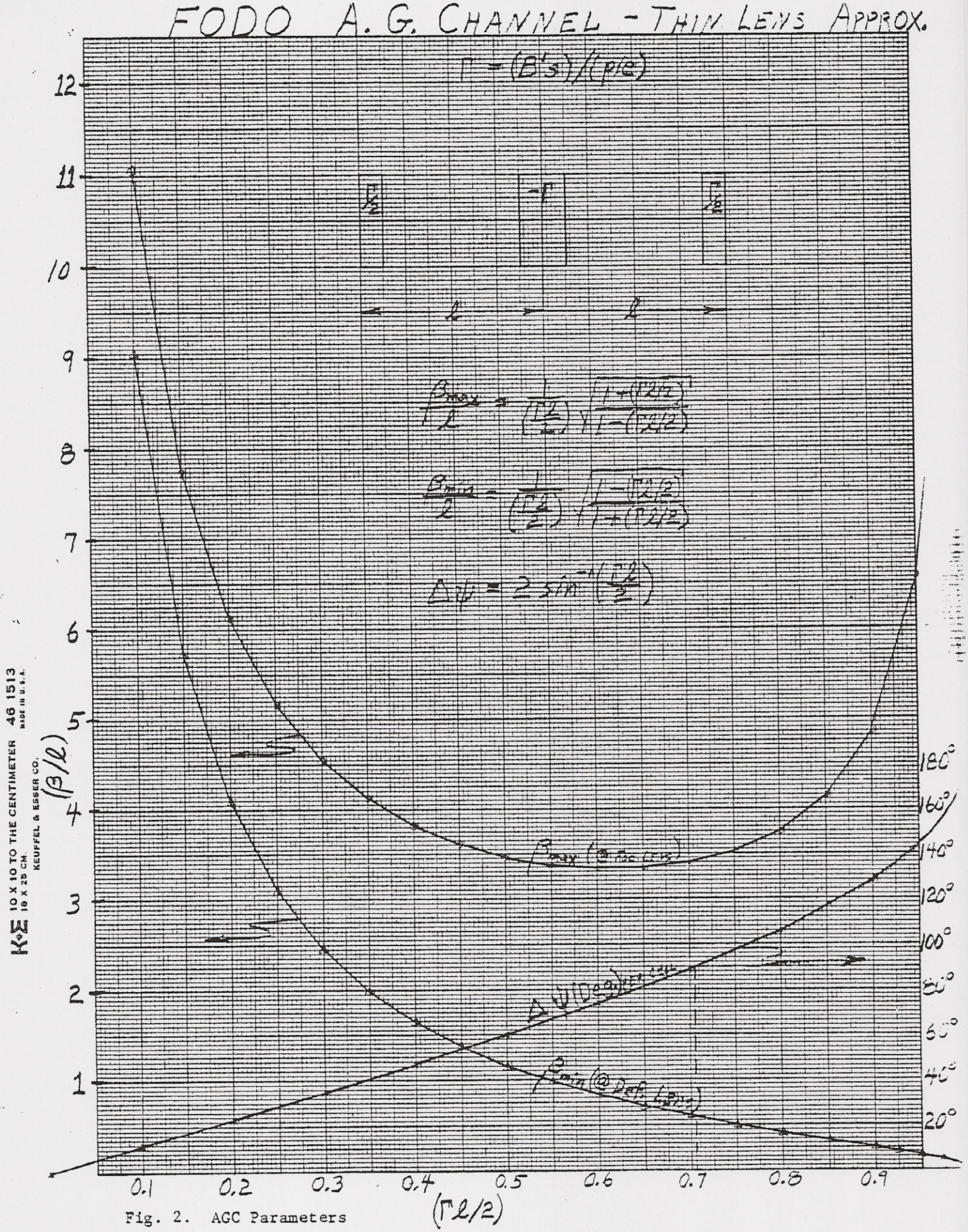

Fig. 2. AGC Parameters

GRAPH PAPER GRAPHIC CONTROLS CORPORATION Buffalo, New York
Printed in U.S.A.
LOGARITHMIC 2 X 3 CYCLES AL-2451-01

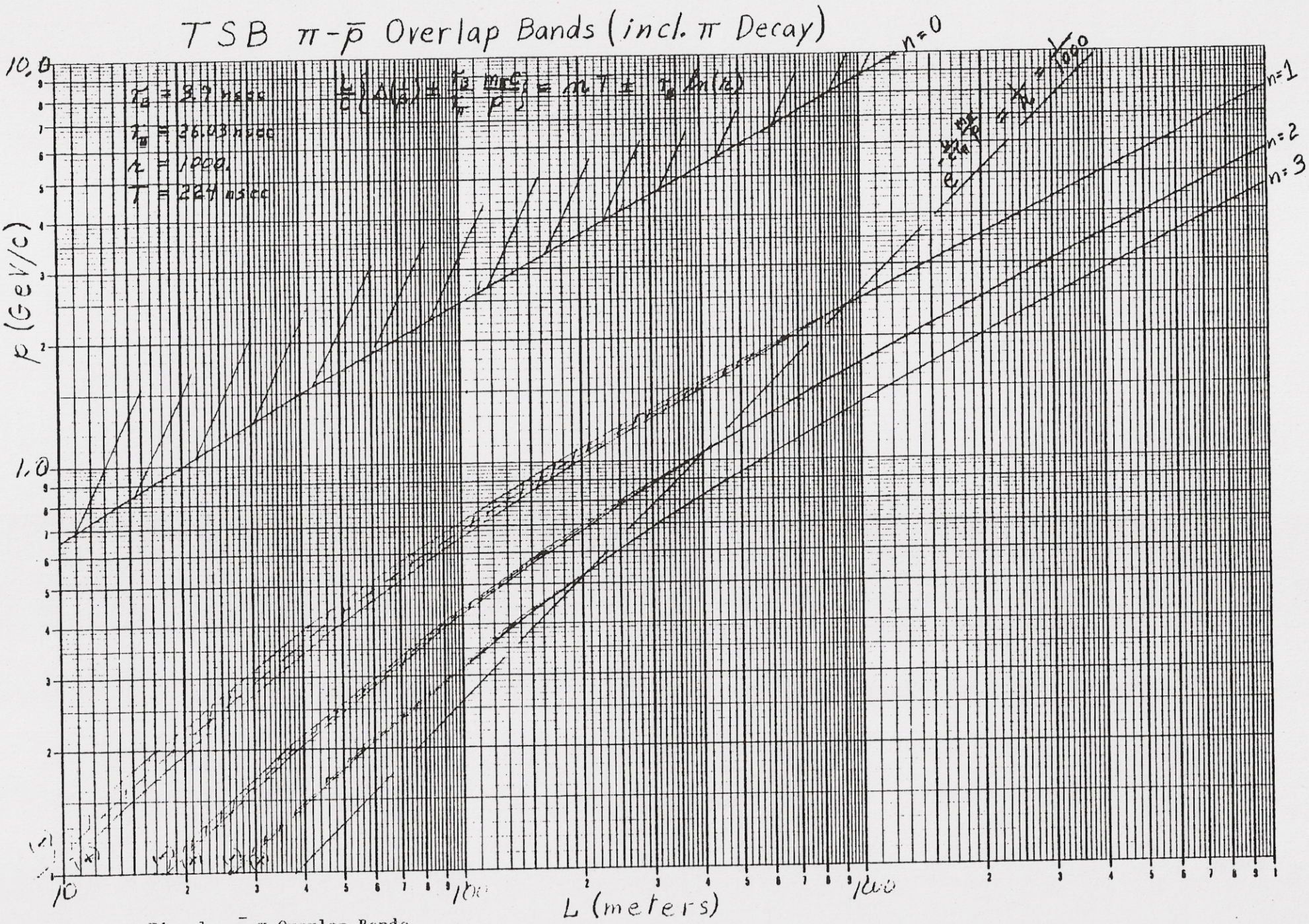

Fig. 1. $\bar{p}$-π Overlap Bands

GRAPH PAPER GRAPHIC CONTROLS CORPORATION Buffalo, New York
Printed in U.S.A.
LOGARITHMIC 2 X 3 CYCLES AL-2451-OF

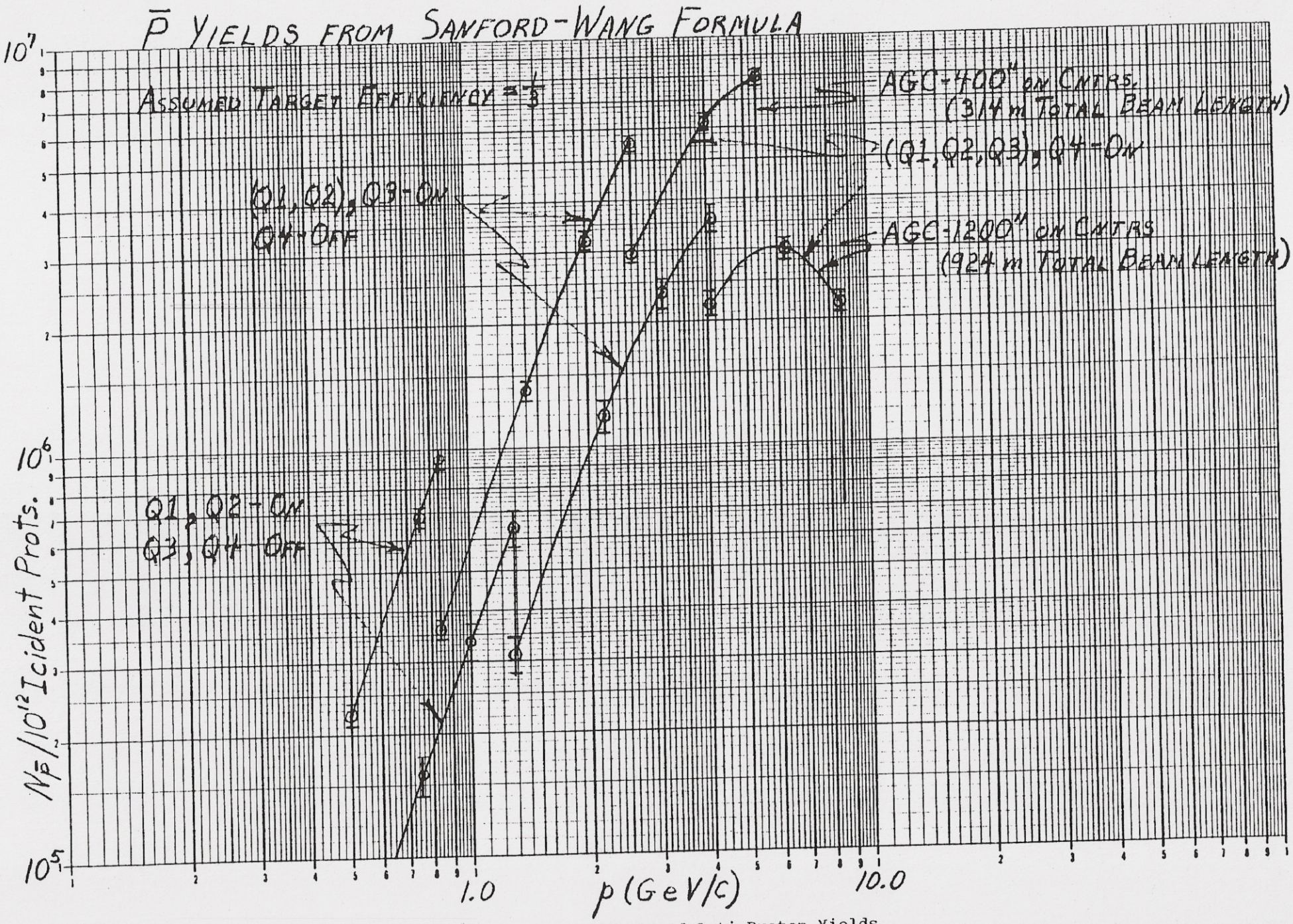

Fig. 6. Calculated Anti-Proton Yields